frontiers | Frontiers in Drug Discovery

TYPE Original Research
PUBLISHED 03 January 2025
DOI 10.3389/fddsv.2024.1459424



OPEN ACCESS

EDITED BY
Ali Kermanizadeh,
University of Derby, United Kingdom

REVIEWED BY
Rodolpho C. Braga,
InsilicAll, Brazil
Seyoum Ayehunie,
MatTek Corporation, United States

*CORRESPONDENCE
Stefanie Hoffmann,
stefanie.hoffmann@merckgroup.com

RECEIVED 04 July 2024
ACCEPTED 19 November 2024
PUBLISHED 03 January 2025

CITATION
Hoffmann S, Hewitt P, Koscielski I, Kurek D, Strijker W and Kosim K (2025) Validation of an MPS-based intestinal cell culture model for the evaluation of drug-induced toxicity.
*Front. Drug Discov.* 4:1459424.
doi: 10.3389/fddsv.2024.1459424



# Validation of an MPS-based intestinal cell culture model for the evaluation of drug-induced toxicity

Stefanie Hoffmann[1]*, Philip Hewitt[1], Isabel Koscielski[1], Dorota Kurek[2], Wouter Strijker[2] and Kinga Kosim[2]

[1]Early Investigative Toxicology, Chemical and Preclinical Safety, Merck Healthcare KGaA, Darmstadt, Germany, [2]MIMETAS B.V., Oegstgeest, Netherlands

**Introduction:** The potential for drug-induced gastrointestinal (GI) toxicity is significant, since the GI tract is one of the first barriers which come in to contact with oral drugs. In pharmaceutical research, the complex behavior of human intestinal cells is traditionally investigated using 2D cultures, in which one cell type grows under static conditions. With the development of advanced microphysiological systems (MPS) more *in vivo* like conditions can be generated which increase the physiological nature and also the predictive validity of these models. Caco-2 cells are known for their capability to build tight junctions. These connections are responsible for the maintenance of intestinal homeostasis and can be used as a specific safety endpoint, by measuring the Trans Epithelial Electrical Resistance (TEER), for the investigation of drug-induced GI toxicity. Compared to a widely used Caco-2 cell 2D Transwell model, the advanced MPS model (Mimetas OrganoPlate®) allows for the recapitulation of the enterocyte cell layer of the intestinal barrier as the Caco-2 cells grow in a tubular structure through which the medium continuously flows.

**Methods:** The OrganoPlate® intestinal model was qualified to be implemented as a routine test system for the early prediction of drug-induced GI toxicity based on the measurement of the tightness of the cell layer by measuring changes in the TEER. For this qualification 23 well known compounds as well as a positive, negative and solvent control were selected. The compounds were selected based on their known effect on the GI system (chemotherapeutics, tight junction disruptor, liver toxins, controls, NSAIDs and a mixed group of drugs).

**Results:** The TEER values were measured 4 h and 24 h after treatment. In parallel the cell viability was determined after 24 h to be able to distinguish between an unspecific cytotoxic effect or direct tight junction damage. Overall, from the 23 tested compounds, 15 showed the expected outcome, i.e., the compound led to a decrease of the TEER for the positive control compounds, or the TEER value remained stable after treatment with non-GI-toxic compounds.

**Conclusion:** In summary, this MPS model allowed the recapitulation of the human intestinal GI barrier and will enable a faster and more robust assessment of drug-induced damage in the GI tract.

KEYWORDS

OrganoTEER, organ-on-chips, *in vitro* barrier model, drug toxicity, CaCo-2, preclinical safety, gastrointestinal-toxicity

# Introduction

Because the gastrointestinal (GI) tract, with its mucus layer, is one of the first barriers that come into contact with external contaminants, toxins, foreign substances, and food, it has an important protective function (Paone and Cani, 2020). A single layer of intestinal epithelial cells (IECs) organized into crypts and villi builds the mucosal surface of the gastrointestinal tract. This monolayer consists of several cell types that differentiate from epithelial stem cells (Soderholm and Pedicord, 2019). These cells separate the gut lumen from the blood and act as a barrier against xenobiotics while allowing the absorption of nutrients (Vancamelbeke and Vermeire, 2017). The tight barrier is mainly generated by polarized absorptive enterocytes connected via different junctional complexes. These connections are divided into tight junctions, adherens junctions, desmosomes, and gap junctions (Turner, 2009).

Damage to the tight junctional complexes increases the paracellular permeability and can lead to tissue damage and, eventually, inflammation (Lee, 2015). This increased permeability can be detected by using a quantitative, non-invasive, label-free, real-time measurement with an impedance-based instrument (Benson et al., 2013). This electrical measurement [trans epithelial electrical resistance (TEER)] is the gold standard for monitoring the barrier function of epithelial cells *in vitro*. Typically, *in vitro* models are used to determine the efficacy and toxicity of new drug candidates as early as possible.

The cultivation of cells on semipermeable membranes enables the generation of two compartments. An electrode is placed in each of the compartments to allow ohmic resistance measurement (Srinivasan et al., 2015; Nicolas et al., 2021). The resulting TEER values are reliable indicators of the barrier integrity.

A classical and widely used method is the measurement of the TEER of a 2D cell monolayer of Caco-2 cells cultured on semipermeable membranes. Caco-2 cells are originally from a human colon adenocarcinoma but express functional and morphological characteristics of differentiated small intestinal enterocytes. They form confluent layers with highly polarized cells, joined via tight junctions, including apical and basolateral sides, with microvilli on the apical membrane (Sambuy et al., 2005). The full differentiation of Caco-2 cells takes approximately 14–21 days on Transwell inserts and reaches TEER values of 150–400 Ω (Srinivasan et al., 2015).

Multiple commercial cell culture models mimic the intestinal barrier (Table 1).

None of them can completely reproduce the complex structure of the human intestine, but each has its benefits and limitations. Microphysiological systems (MPS) and organ-on-a-chip (OoC) systems allow the combination of several parameters, such as extracellular matrices (ECM), three-dimensional (3D) growing of cells, nutrient flow including shear stress, and co-culture options. By an improved mapping of the *in vivo* environment, 3D models can help to better select drug candidates and can reduce costs by improving the prediction of drug efficacy and toxicity (Peng et al., 2017).

A good combination of complexity and throughput can be created with the Mimetas OrganoPlate® 3-lane, and that system was chosen for this study. This system includes cells that grow against an ECM in a 3D tubular structure. The nutrient supply is generated by a bidirectional flow of media. The main goal of this study was to investigate the OrganoPlate and how it can be used for early routine testing of potential drug-induced GI toxicity. If successful, the OrganoPlate will be implemented into early preclinical development to test a variety of drug candidates for their potential to cause direct toxicity to the small intestine.

# Materials and methods

## Cell culture and seeding of cells

The human colon carcinoma cell line Caco-2 (Sigma-Aldrich, 86010202) was cultured in T175 flasks in DMEM 4.5 g/L glucose (Lonza, 12-614F), 10% FBS (Gibco, 102070-106), 1% penicillin/streptomycin (Sigma, P4333) and 1% L-glutamine (Gibco, 25030-081). Caco-2 cells were harvested between passage 3 and 20 for experiments. The cells were cultured at 37°C and 5% $CO_2$, and the medium was refreshed every 2–3 days. At 70%–80% confluency, the cells were either sub-cultured or used for experiments.

Cells were trypsinized using Trypsin-EDTA solution (Sigma-Aldrich, T3924) and resuspended at 10,000 cells per µl prior to seeding. The cells were applied to 3-lane OrganoPlates (Mimetas, 4004-400-B). Prior to cell seeding, 1.7 µL of a gel composed of 1 M Hepes (Gibco, 15630-080), 37 g/L $NaHCO_3$ (Sigma, S5761), and 4 mg/mL Collagen I (R&D System, 3447-020-01) in a 1:1:8 ratio was added in the gel inlet and incubated for 15 min at 37°C. After polymerization, 50 µL HBSS (Cytiva, SH30268.01) was dispensed in the gel inlet channels to avoid dehydration of the gel. The cells were applied by seeding 2 µL of $1 \times 10^7$ cells/mL cell suspension in the inlet of the top channel. Subsequently, 50 µL of medium was added to the same well. Afterward, the OrganoPlate was placed on its side on a specific plate stand for 4 h at 37°C to allow the cells to settle against the ECM. This was followed by adding an additional 50 µL medium to the outlets of the top channel and to the inlets and outlets of the bottom channel. Next, the OrganoPlate was placed horizontally in an incubator (37°C and 5% $CO_2$) on an interval rocker (OrganoFlow, Mimetas), which switches the inclination between +7° and −7° every 8 min and allows a bidirectional flow of the medium. Every 2–3 days, the medium was refreshed.

The 3-lane OrganoPlate® contains 40 chips, each of which has three microfluidic channels, and all are based on a 384-well plate

10.3389/fddsv.2024.1459424

TABLE 1 Overview of commercially available cell culture models for the intestinal tract (non-exhaustive).

| | Model | | | | | | | |
|---|---|---|---|---|---|---|---|---|
| | Caco-2 | Caco-2 & HT29 | Organoids | RepliGut® | Mimetas OrganoPlate® | EpiIntestinal™ 3D | Ussing chamber | Animals |
| | *In vitro* | *In vitro* | *In vitro* | *In vitro* | *In vitro* | *In vitro* | *Ex vivo* | *In vivo* |
| Source | Human cancer cell line | Human cancer cell lines | Human iPSC or adult stem cells | Human, primary | Human cancer cell line | Human, small intestine epithelial, and endothelial cells | Animal tissue explant | Complete animal |
| Cell types | Monoculture of Caco-2 | Co-culture of Caco-2 & HT29-MTX | Multiple cells (primary or adults/iPS cells) | Multiple cells (colon or small intestine) differentiated from stem cells | Monoculture of Caco-2 | Multiple (enterocytes, Paneth cells, tuft cells, M cells, and stem cells) | Multiple species | All cells from an animal |
| Platform | Transwell | Transwell | Flat plate | Transwell | 3-lane OrganoPlate | Transwell | — | — |
| Flow | No | No | No | No | Yes | No | No | Yes |
| ECM | No | No | Yes (Matrigel) | No | Yes (Collagen) | Yes | No | Yes |
| Pre-preparation time[a] | 21 days | 21 days | ~6–10 days | 14–17 | 4–6 days | Up to 14 days (MatTek Corp.) | Animal growth | Animal growth |
| Pros | - Inexpensive<br>- Easy handling | - Inexpensive<br>- Easy handling | - 3D<br>- Presence of important cell types from the tissue | Proliferative stem cells | - Flow introduces sheer stress and nutrient transport<br>- Compatible with commercial plate reader | - Forms villi, microvilli, brush borders, and tight junctions<br>- Cultivation up to 42 days<br>- Organotypic small intestinal tissue reconstruction | - Barrier of animal tissue | - Complex structure<br>- Cell–cell contact and organ interaction<br>- complete organism (DNA) |
| Cons | - Cancer cell line<br>- 2D | - Cancer cell line<br>- 2D | - High deviations | - Needs training | - Needs training | - Needs training | - Needs animals<br>- Analysis of a small set of segments of epithelial tissue<br>- Low throughput | - Animal experiment<br>- Expensive<br>- Time intensive<br>- Ethical reasons<br>-lack of applicability |
| Supplier | ATCC & others | ATCC & others | Several | Altis biosystem | Mimetas | MatTek | Reprocell and others | Several |
| Costs | $ | $ | $$ | $$$$ | $$ | $$$ | $$- $$$ | $$$$$ |
| Reference | Sambuy et al. (2005) | Walter et al. (1996) | Zhang et al. (2021) | Lemmens et al. (2021) | Trietsch et al., 2017; Nicolas et al. (2021) | Ayehunie et al. (2013) | Thomson et al. (2019) | Crystal, (2018) |

[a]Pre-preparation time, time for pre-cultivation of animals/cells for experiments.

format. Each chip contains two perfusion channels and one channel for an extracellular matrix (Figure 1). Compared to commonly used 2D models, it has a shorter pre-cultivation time (2D Transwell: 14–21 days until polarized Caco-2 cells and OrganoPlate: 4–6 days), more complexity (3D tube of cells, ECM, media flow), and allows the measurement of the TEER of 40 chips in parallel.

## Treatment of cells

Caco-2 cells in OrganoPlates were exposed to test compounds (Table 2) for 24 h. Three different concentrations were tested for each compound. For the treatment, the medium was completely removed, and 50 µL of compound-medium solution was added in each inlet and outlet of the top channel. Compounds were selected based on the occurrence of side effects in the GI tract or based on the specific occurrence of tight junction damage. Compound concentrations were chosen based on literature values and already-published data with Caco-2 cells in 2D. Each compound was tested three times.

## TEER measurement

The TEER of the Caco-2 cultures in the OrganoPlate was measured by using an automated multichannel impedance spectrometer (OrganoTEER, Mimetas). TEER was measured

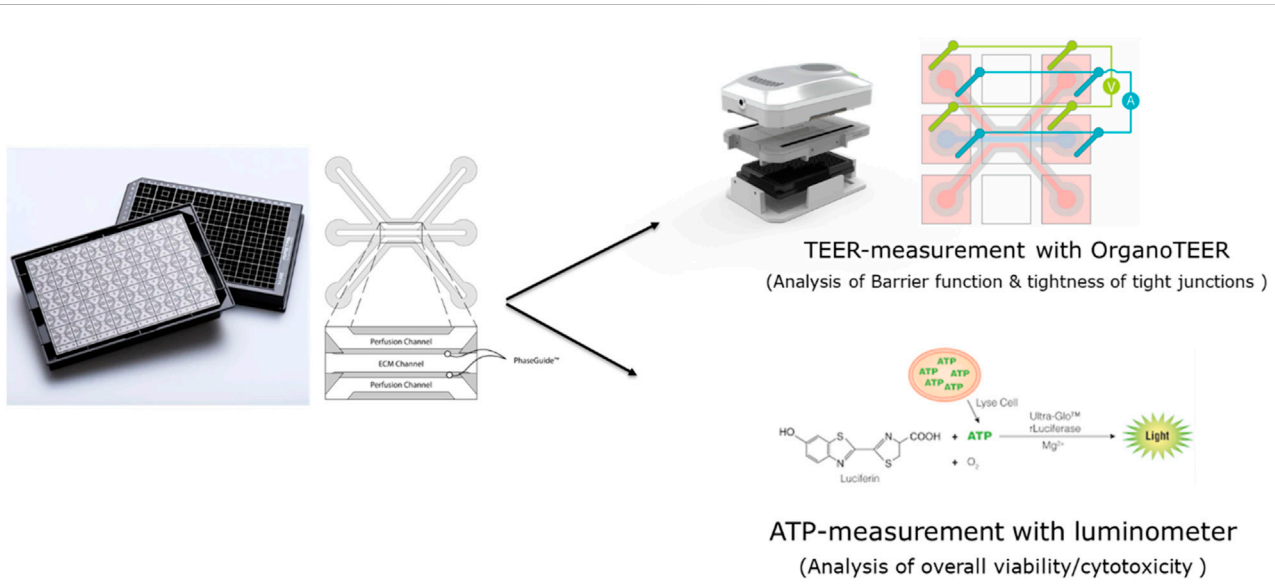


FIGURE 1
Schematic overview of the OrganoPlate 3-lane and the assays performed in this study.

before treatment (0 h), 4 h after treatment (4 h), and 24 h after treatment (24 h). Before the measurement, a medium exchange of 50 µL medium was performed in the inlets and outlets of the middle channel, and then the OrganoPlate was equilibrated for 30 min at RT. The electrode board of the OrganoTEER fits in the OrganoPlate and introduces the electrodes in the medium of all inlet and outlet wells connecting to the apical and basal side of the Caco-2 tubes.

Before each measurement, the electrode board was cleaned by spraying 70% ethanol onto the board. Under a laminar flow, the electrode was left to dry for at least 30 min. Between each experimental run, the electrode board was immersed in a single well plate filled with 50 mL of a 1:20 solution of RBS T342 (Chemical Products R. Borghgraef N.V, BE) in Milli-Q-Water. The electrode board was left in the solution for 15–20 min, and afterward, the electrode board was rinsed with Milli-Q-Water and left to dry ambiently.

## ATP measurement

To quantify the number of viable cells, the CellTiter-Glo® 3D (Promega, G9681) assay was used, which determines the amount of intracellular ATP and is indicative of the number of metabolically active cells. A 25 µL aliquot of CellTiter-Glo® 3D reagent was added in each inlet and outlet of the top channel. The OrganoPlates were placed on a shaker for 5 min, 300 rpm in the dark, and then left for 25 min. The luminescence signal was immediately read in a luminometer.

## Data analysis and statistics

Data from the OrganoTEER were analyzed using the OrganoTEER software and MS Excel to calculate the change in TEER values at 4 h and 24 h, which were reported as a percentage of initial TEER values.

# Results

The selected compounds were divided into six subclasses (controls, NSAIDs, chemotherapeutics, liver toxins, tight junction disruptors, and a mixed group of compounds) according to their reported effect (Table 3). Compounds were selected based on their effect *in vivo* or on Caco-2 cells. Compound concentrations were selected based on given concentrations that showed toxic effects from the literature.

In prior experiments (data not shown), the OrganoPlates® was shown to generate a stable TEER value after 6 days. For internal validation of the OrganoPlate and the use of the OrganoTEER for the measurement of the tightness of the cell barriers, 23 well-known compounds were used to treat the Caco-2 cells.

## Characterization of Caco-2 cells in the OrganoPlate

After seeding the Caco-2 cells in the top channel inlet, the cells start to grow against the extracellular matrix, which is made of collagen I. The cells grew in a tubular structure within 4 days (Figure 2) and formed a tight monolayer. The staining with the antibodies claudin 7 and E-cadherin indicates an undisrupted appearance of tight junctions, which is correlated to a tight barrier function (Figure 3).

## TEER measurements after test compound exposure

We assessed the barrier function of Caco-2 tubes in response to the control compounds (staurosporine and metformin) and to the test compounds, which are listed above (Table 2). Staurosporine, a protein kinase C inhibitor that induces apoptosis, is known to

TABLE 2 Reference compounds used for testing the usability of the OrganoPlate to predict well-known GI toxicity.

| Compound | Manufacturer | Catalog number |
|---|---|---|
| Ibuprofen | Cayman Chemicals | 70280 |
| Indomethacin | Sigma-Aldrich | I7378 |
| Diclofenac | Sigma-Aldrich | SML3086 |
| 5-Fluorouracil | Sigma-Aldrich | F6627 |
| Alosetron | Cayman Chemicals | 22434 |
| Irinotecan hydrochloride | abcr | AB252173 |
| Sunitinib | Sigma-Aldrich | PZ0012 |
| Sorafenib | Sigma-Aldrich | SML2653 |
| Flavopiridol | Cayman Chemicals | 10009197 |
| Bortezomib | VWR | 5.04314.0001 |
| Bosutinib | Sigma-Aldrich | PZ019 |
| Carboplatin | Cayman Chemicals | Cay13112 |
| Docetaxel | Cayman Chemicals | Cay11367 |
| Afatinib | LKT Laboratories | LKT-A2077.5 |
| Troglitazone | Cayman Chemicals | 71750 |
| Trovafloxacin | Sigma-Aldrich | PZ0015 |
| Homoharringtonine | Sigma-Aldrich | SML1091 |
| Patulin | VWR | 5.04314.0001 |
| Phenylarsine oxide | VWR | A14674.03 |
| Sodium orthovanadate | Sigma-Aldrich | 567540 |
| Duloxetine | Sigma-Aldrich | SML0474 |
| Terfenadine | Sigma-Aldrich | T9652 |
| Loperamide hydrochloride | LKT Laboratories | L5660 |
| Staurosporine | abcr | AB353975 |
| Metformin hydrochloride | Sigma-Aldrich | PHR1084 |

disrupt the epithelial barrier and was selected as a positive control, and metformin, which is used for the treatment of type 2 diabetes, was used as the negative control.

The positive control staurosporine led to a reduction of the TEER value at 4 h after treatment at all tested concentrations (100 µM, 10 µM, 1 µM) but with a more-reduced TEER after 24 h of treatment (Figure 4A). The viability results showed a dose-dependent decrease in viability 24 h after treatment with staurosporine (Figure 4B). Compared to this, the TEER values for metformin and DMSO remained stable after 4 h and 24 h, and the viability of the cells remained at approximately 100% after 24 h (Figures 4A, B).

The reference compounds were tested at three concentrations selected based on already-published data or previous internal experiments. Based on their field of application, the compounds were subdivided into six compound classes (NSAIDs, chemotherapeutics, tight junction disruptors, a mixed group, liver toxins, and control compounds).

Of the NSAIDs tested, ibuprofen did not influence the tight junctions or the viability of the cells. Treatment with indomethacin led to a decrease of the TEER at the highest concentration tested (500 µM) without a decrease in viability (Supplementary Figure 1). Diclofenac damaged the tight junctions and reduced the viability after treatment with the two highest concentrations (2,000 µM and 1,000 µM) (Figure 5). The results for the TEER and viability experiments clearly show a dose-dependent toxicity of diclofenac.

Treatment with phenylarsine oxide, patulin, and homoharringtonine at the highest concentration caused damage to the tight junctions, resulting in a lower TEER value than the vehicle control, DMSO. Following the treatment with patulin and homoharringtonine, the TEER value also decreased at the lower concentrations tested (Figure 6A). From all the tight junction disruptors tested, patulin and phenylarsine oxide showed the strongest cytotoxicity with residual survival at approximately 0%–20% at the highest concentration tested (100 µM and 5 µM, respectively) (Figure 6A). The TEER values decreased up to 80% after the cells were treated with both compounds. After treatment, the viability of the cells with the highest concentration of patulin and phenylarsine oxide also decreased after 24 h (Figure 6B). Sodium orthovanadate showed no toxic effect on the tight junctions or the vitality of the Caco-2 cells (Supplementary Figure 3).

Troglitazone and trovafloxacin showed no decrease in the TEER values and no decrease in viability. All Caco-2 tubes remained intact, and the cells were not affected by both liver toxic compounds (Figure 7).

In this validation study, most of the tested chemotherapeutic drugs did not show a relevant drop in the TEER value. Exposure to 5-FU, alosetron, irinotecan, sunitinib, sorafenib, and carboplatin did not lead to a decrease of the TEER value nor to a decrease in viability (Supplementary Figures 5, 6). Exposure to the highest concentration (300 µM) of flavopiridol leads to damage of the tight junctions with a subsequent decrease of the TEER value (approximately 60%), but the cells remained viable at this concentration (Supplementary Figure 4). Exposure to bortezomib led to a decrease of the TEER value of a minimum of 70%, at least in the highest concentration, and bosutinib appeared to cause direct cytotoxicity and impacted the tight junctions, resulting in a simultaneous decrease in TEER and induction of cell death at 50 µM and 25 µM (Figures 8A, B).

The three compounds from the mixed group, loperamide, duloxetine, and terfenadine, showed a decreased TEER value at the highest concentration tested, and the viability decreased (Supplementary Figure 2). A summary of all results is shown in Table 4.

In addition to these results, data from previous 2D Transwell studies were used to compare these with the results from this study to evaluate whether the OrganoPlate® could help to better predict potential side effects of drug candidates on the intestinal barrier compared to the traditional Transwell models. For these studies, Caco-2 cells were seeded onto semipermeable membranes of Transwell inserts, creating two compartments that mimic the intestinal barrier (Awortwe et al., 2014), (Figure 9). The cells were cultivated for 21 days until they reached a confluent monolayer of >150 $\Omega^*cm^2$. The cells were then treated with test compounds, and TEER values were determined after 24 h. Overall, nine test compounds (two NSAIDs, four chemotherapeutics, one liver toxin, and two from the mixed group) were used in the

TABLE 3 Overview of the selected reference compounds used for the qualification of the OrganoPlate and the use of the OrganoTEER to predict GI toxicity *in vitro*.

| Compound class | Compound name | MoA/toxicity | Side effects in the human GI tract | Reference |
|---|---|---|---|---|
| Controls | Metformin | Type 2 diabetes mellitus drug, lowers glucose production in the liver and increases glucose utilization in the gut | In adequate amounts: diarrhea, nausea, vomiting, and abdominal discomfort | Bonnet and Scheen (2017), Rena et al. (2017), and Peters et al. (2019) |
| | Staurosporine | Strong protein kinase and cyclin-dependent kinase inhibitor, induces cell cycle arrest | No side effects known for the GI tract | Oikawa et al. (1992); Antonsson and Persson (2009), and Trietsch et al., 2017 |
| NSAID | Ibuprofen | Inhibition of prostaglandin synthesis, antibody synthesis, cytokine production, transcription factors, and inhibition of leukocyte functions; apoptosis | Abdominal pain, nausea, and diarrhea | Rampal et al. (2002) and Rainsford (2009) |
| | Diclofenac | Inhibition of prostaglandin synthesis COX-inhibitor | Bleeding, inflammation, and ulceration in SI; nausea, vomiting, diarrhea, dyspepsia, and abdominal pain; rare: hemorrhage, gastrointestinal ulcer, colitis, and constipation | Bhatt et al. (2018) |
| | Indomethacin | Inhibition of prostaglandin synthesis, COX-inhibitor | Bleeding, ulceration, perforation of stomach or intestine, and lesions in the small intestine | Maseda and Ricciotti (2020) |
| Chemotherapeutics | 5-Fluorouracil | Toxic effect on specific proteins of the tight junctions in immunodeficient mice, specifically on occludin and claudin-1. Both proteins are also found in the human intestine and have also been detected in Caco-2 cells; cell death | Intestinal injury, epithelial ulceration in the mucosa (mucositis), which manifests mainly in pain and dyspeptic syndromes or inflammation; damage of intestinal barrier function, reduced enterocyte proliferation, and crypt cell apoptosis | Soares et al. (2013), Song et al. (2013), and Garcia-Hernandez et al. (2017) |
| | Alosetron | Highly potent 5-HT3 receptor antagonist that improves abdominal pain and can slow colonic transit | Constipation, ischemic colitis, and death | Peters et al. (2019) |
| | Irinotecan | Accumulation of SN-38 metabolite in the enterocytes; SN-38 inhibits the DNA topoisomerase I by inducing DNA damage in tumor cells and accumulation in the intestinal mucosa | Nausea, vomiting, abdominal pain, and constipation | Lee et al. (2014), Wardill et al. (2014), and EMC (2018) |
| | Sunitinib | Tyrosine kinase inhibitor; used for the treatment of renal carcinoma and gastrointestinal stromal tumors | Nausea, vomiting, and indigestion | Le Tourneau et al. (2007), Durand et al. (2012), and Sehdev (2016) |
| | Sorafenib | Tyrosine kinase inhibitor | Diarrhea; decrease in TEER and plasma citrulline (Caco-2) | Durand et al. (2012) |
| | Flavopiridol | Inhibits cyclin-dependent kinases and blocks cell cycle progression | Diarrhea, nausea, and vomiting | Senderowicz (1999), Byrd et al. (2007), and William et al. (2010) |
| | Bortezomib | Proteasome inhibitor | Nausea, vomiting, constipation, and diarrhea | Sun et al. (2005) and Peters et al. (2019) |
| | Bosutinib | Tyrosine kinase inhibitor<br>Decrease TEER | Nausea, vomiting, and bleeding | Khoury et al. (2012), French (2019), and Peters et al. (2019) |
| | Carboplatin | Apoptosis inducer, DNA crosslinker | Nausea and vomiting | Peters et al. (2019) |
| | Docetaxel | Taxane, disrupts the normal function of microtubules | Nausea, vomiting, enterocolitis, perforation, colitis, and diarrhea | Ho and Mackey (2014) and Peters et al. (2019) |
| | Afatinib | EGFR inhibitor | Diarrhea | Peters et al. (2019) |
| Liver toxins | Troglitazone | Liver tox | No side effects known for the GI tract | — |
| | Trovafloxacin | Liver tox | No side effects known for the GI tract | — |
| Tight junction damager | Phenylarsine oxide | PTP inhibitor, which is a key mediator of intestinal epithelial barrier function | In humans: decrease in the surface area of the GI tract, change in TEER | Rao et al. (1997) and Mahfoud et al. (2002) |

(Continued on following page)

TABLE 3 (*Continued*) Overview of the selected reference compounds used for the qualification of the OrganoPlate and the use of the OrganoTEER to predict GI toxicity *in vitro*.

| Compound class | Compound name | MoA/toxicity | Side effects in the human GI tract | Reference |
|---|---|---|---|---|
| | | Caco-2: downregulation of ZO-1, disruption of claudins leads to tight junction; decrease in TEER | | |
| | Sodium orthovanadate | Inhibitor of protein tyrosine phosphatases, alkaline phosphatase, and ATPase, disrupts the tight junctions | Increases intestinal epithelial permeability and changes homeostasis | Rao et al. (1997) and Kim et al. (2022) |
| | Homoharringtonine | Inhibits protein synthesis (ribosomes) of cancer cells | Increases intestinal epithelial permeability (Caco-2) and reduces tight junction barrier (Caco-2) | Zhou et al. (1995) and Watari et al. (2015) |
| | Patulin | Mycotoxin, alters intestinal barrier function | Induces intestinal injuries, including epithelial cell degeneration, inflammation, ulceration, and hemorrhages; decrease TEER (Caco-2) | Mahfoud et al. (2002) |
| Mixed group | Duloxetine | Inhibits the reuptake of serotonin and norepinephrine (NE) in the central nervous system | Nausea, vomiting, and constipation | Peters et al. (2019) |
| | Loperamide | Opiate agonist, inhibits the action of calmodulin | Bloating, nausea, vomiting, and constipation | Mellstrand (1987) and Hanauer (2008) |
| | Terfenadine | Prolongation of the QT interval | Nonspecific | Roden, (2019) |
| Controls | Metformin | Type 2 diabetes mellitus drug; lowers glucose production in the liver and increases glucose utilization in the gut | In adequate amounts: diarrhea, nausea, vomiting, and abdominal discomfort | Bonnet and Scheen (2017), Rena et al. (2017), and Peters et al., 2019 |
| | Staurosporine | Strong protein kinase and cyclin-dependent kinase inhibitor, induces cell cycle arrest | No side effects known for the GI tract | Oikawa et al. (1992), Antonsson and Persson (2009), and Trietsch et al. (2017) |
| NSAID | Ibuprofen | Inhibition of prostaglandin synthesis, antibody synthesis, cytokine production, transcription factors, and inhibition of leukocyte functions; apoptosis | Abdominal pain, nausea, and diarrhea | Rampal et al. (2002) and Rainsford (2009) |
| | Diclofenac | Inhibition of prostaglandin synthesis COX-inhibitor | Bleeding, inflammation, and ulceration in SI; nausea, vomiting, diarrhea, dyspepsia, and abdominal pain; rare: hemorrhage, gastrointestinal ulcer, colitis, and constipation | Bhatt et al. (2018) |
| | Indomethacin | Inhibit prostaglandin synthesis, COX-inhibitor | Bleeding, ulceration, perforation of stomach or intestine, and lesions in the small intestine | Maseda and Ricciotti (2020) |
| Chemotherapeutics | 5-Fluorouracil | Toxic effect on specific proteins of the tight junctions in immunodeficient mice, specifically on occludin and claudin-1. Both proteins are also found in the human intestine and have also been detected in Caco-2 cells; cell death | Intestinal injury, epithelial ulceration in the mucosa (mucositis), which manifests mainly in pain and dyspeptic syndromes or inflammation; damage of intestinal barrier function, reduced enterocyte proliferation, and crypt cell apoptosis | Soares et al. (2013), Song et al. (2013), and Garcia-Hernandez, et al. (2017) |
| | Alosetron | Highly potent 5-HT3 receptor antagonist that improves abdominal pain and can slow down colonic transit | Constipation, ischemic colitis, and death | Peters et al. (2019) |
| | Irinotecan | Accumulation of SN-38 metabolite in the enterocytes; SN-38 inhibits the DNA topoisomerase I by inducing DNA damage in tumor cells and accumulation in intestinal mucosa | Nausea, vomiting, abdominal pain, and constipation | Lee et al. (2014), Wardill et al. (2014), and EMC (2018) |
| | Sunitinib | Tyrosine kinase inhibitor; used for the treatment of renal carcinoma and gastrointestinal stromal tumors | Nausea, vomiting, and indigestion | Le Tourneau et al. (2007), Durand et al. (2012), and Sehdev (2016) |

(Continued on following page)

10.3389/fddsv.2024.1459424

**TABLE 3** (*Continued*) Overview of the selected reference compounds used for the qualification of the OrganoPlate and the use of the OrganoTEER to predict GI toxicity *in vitro*.

| Compound class | Compound name | MoA/toxicity | Side effects in the human GI tract | Reference |
|---|---|---|---|---|
| | Sorafenib | Tyrosine kinase inhibitor | Diarrhea; decrease in TEER and plasma citrulline (Caco-2) | Durand et al. (2012) |
| | Flavopiridol | Inhibits cyclin-dependent kinases and blocks cell cycle progression | Diarrhea, nausea, vomiting | Senderowicz (1999), Byrd et al. (2007), and William et al. (2010) |
| | Bortezomib | Proteasome inhibitor | Nausea, vomiting, constipation, and diarrhea | Sun et al. (2005) and Peters et al. (2019) |
| | Bosutinib | Tyrosine kinase inhibitor<br>Decrease TEER | Nausea, vomiting, and bleeding | Khoury et al. (2012), French (2019), and Peters et al. (2019) |
| | Carboplatin | Apoptosis inducer, DNA crosslinker | Nausea and vomiting | Peters et al. (2019) |
| | Docetaxel | Taxane, disrupts the normal function of microtubules | Nausea, vomiting, enterocolitis, perforation, colitis, and diarrhea | Ho and Mackey (2014) and Peters et al. (2019) |
| | Afatinib | EGFR inhibitor | Diarrhea | Peters et al. (2019) |
| Liver toxins | Troglitazone | Liver tox | No side effects known for the GI tract | — |
| | Trovafloxacin | Liver tox | No side effects known for the GI tract | — |
| Tight junction damager | Phenylarsine oxide | PTP inhibitor, which is a key mediator of intestinal epithelial barrier function<br>Caco-2: downregulation of ZO-1, disruption of claudins leads to tight junction; decrease in TEER | In humans: decrease in the surface area of the GI tract, change in TEER | Rao et al. (1997) and Mahfoud et al. (2002) |
| | Sodium orthovanadate | Inhibitor of protein tyrosine phosphatases, alkaline phosphatase, and ATPase, disrupt the tight junctions | Increases intestinal epithelial permeability and changes homeostasis | Rao et al. (1997) and Kim et al. (2022) |
| | Homoharringtonine | Inhibits protein synthesis (ribosomes) of cancer cells | Increases intestinal epithelial permeability (Caco-2) and reduces tight junction barrier (Caco-2) | Zhou et al. (1995) and Watari et al. (2015) |
| | Patulin | Mycotoxin, alters intestinal barrier function | Induces intestinal injuries, including epithelial cell degeneration, inflammation, ulceration, and hemorrhages; decrease TEER (Caco-2) | Mahfoud et al. (2002) |
| Mixed group | Duloxetine | Inhibits the reuptake of serotonin and norepinephrine (NE) in the central nervous system | Nausea, vomiting, and constipation | Peters et al. (2019) |
| | Loperamide | Opiate agonist, inhibits action of calmodulin | Bloating, nausea, vomiting, and constipation | Mellstrand (1987) and Hanauer (2008) |
| | Terfenadine | Prolongation of the QT interval | Nonspecific | Roden (2019) |

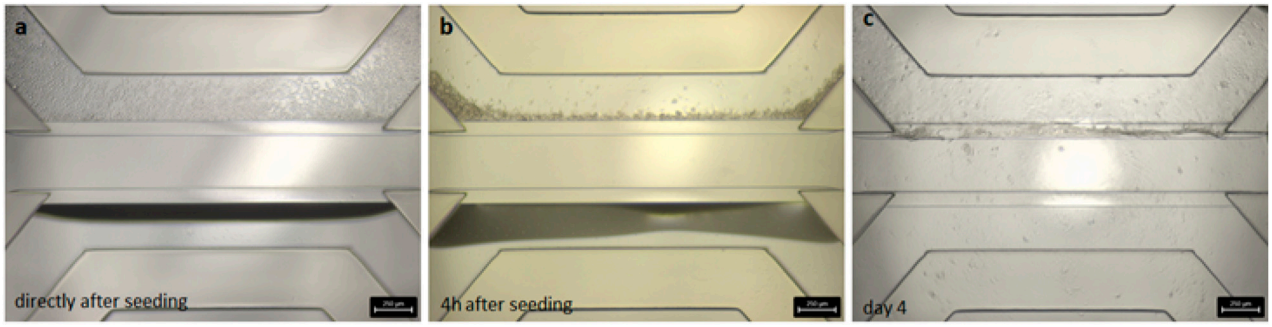


FIGURE 2
Brightfield images of the seeded Caco-2 cells in the OrganoPlate® 3-lane. **(A)** Cell distribution within the chip directly after seeding. **(B)** Cell sedimentation against the collagen layer after 4 h of attachment time. **(C)** Confluent cell layer visible after 4 days cultivation on the rocker.

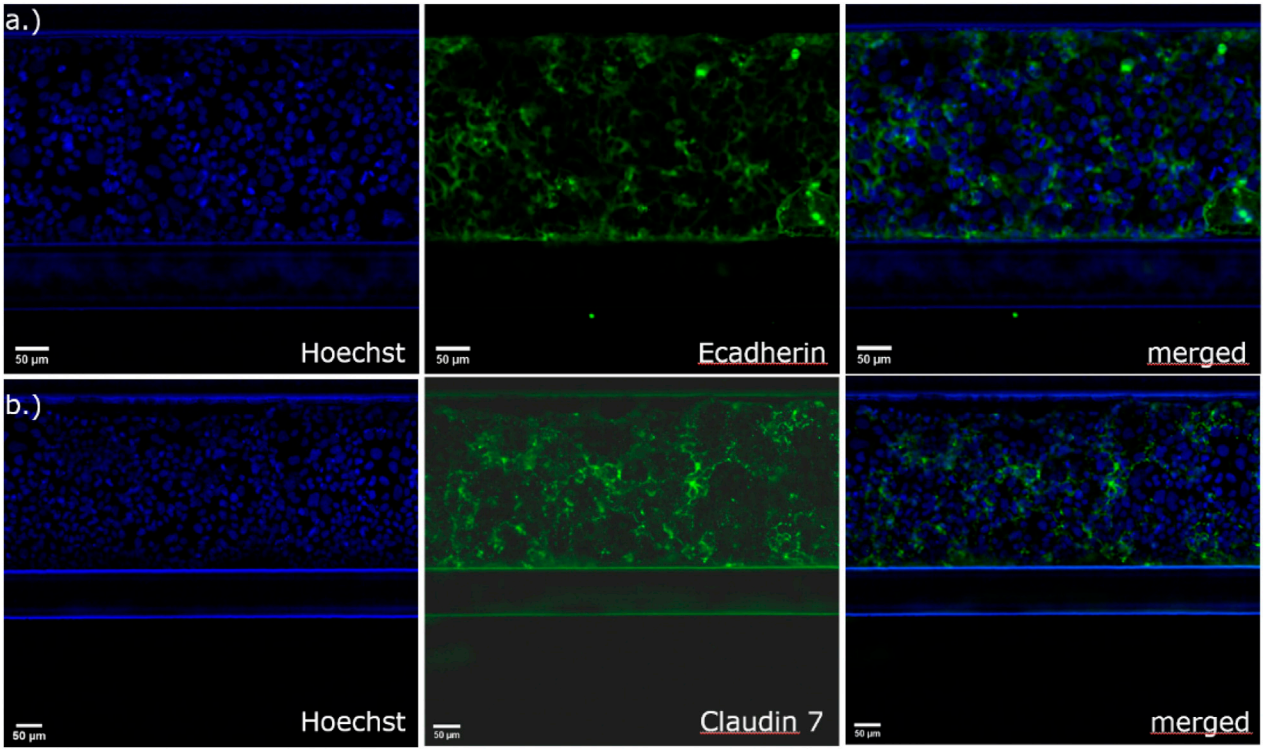


FIGURE 3
Immunofluorescence staining with **(A)** E-cadherin for the detection of adherens junctions and **(B)** claudin-7 for the detection of tight junctional complexes in Caco-2 cells in the 3-lane OrganoPlate®.

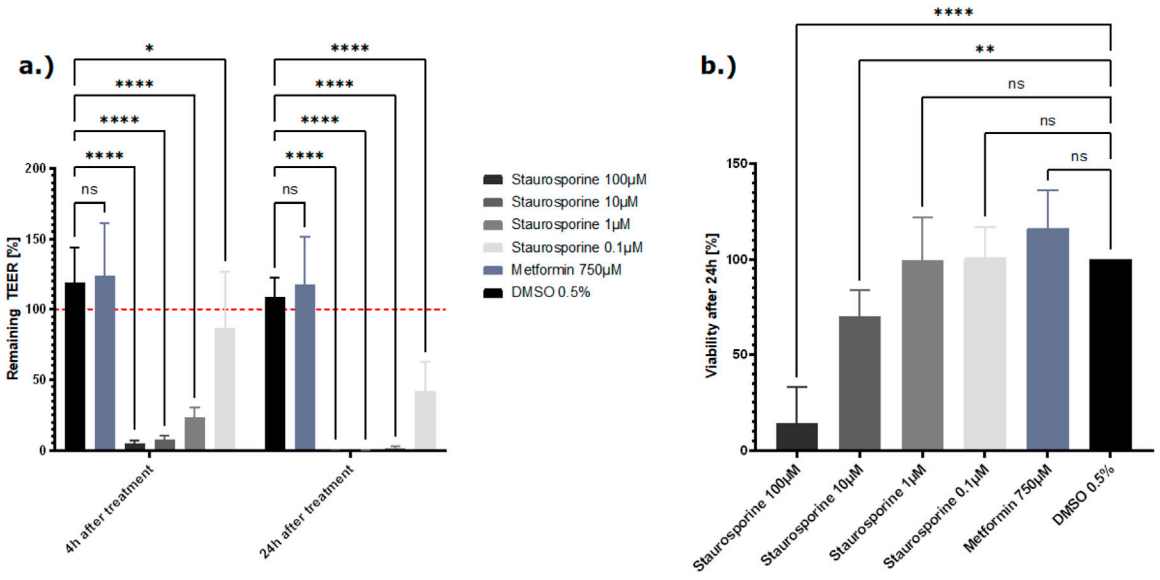


FIGURE 4
**(A)** Effect of the control compounds on the barrier function shown as the percentage change relative to the TEER value at t0 of the treatment. TEER values were measured after treatment with the positive control staurosporine, vehicle control DMSO, and the negative control metformin. The mean TEER values 4 h and 24 h after treatment are shown. The dotted red line shows the normalized initial TEER values of 100%. **(B)** The effect of the control compounds on the cell viability is shown as a % change to the DMSO control. Viability was measured with the CellTiter-Glo 3D kit 24 h after treatment with staurosporine, DMSO, and metformin. The data are presented as means ± SD (n = 8, statistical analysis of TEER values: ****$p < 0.0001$ and **$p = 0.0013$ by two-way ANOVA with Dunnett's test for multiple comparisons to the control. For statistical analysis of viability values: ****$p < 0.0001$ and ***$p = 0.0037$ by one-way ANOVA with Dunnett's test for multiple comparisons to the control).

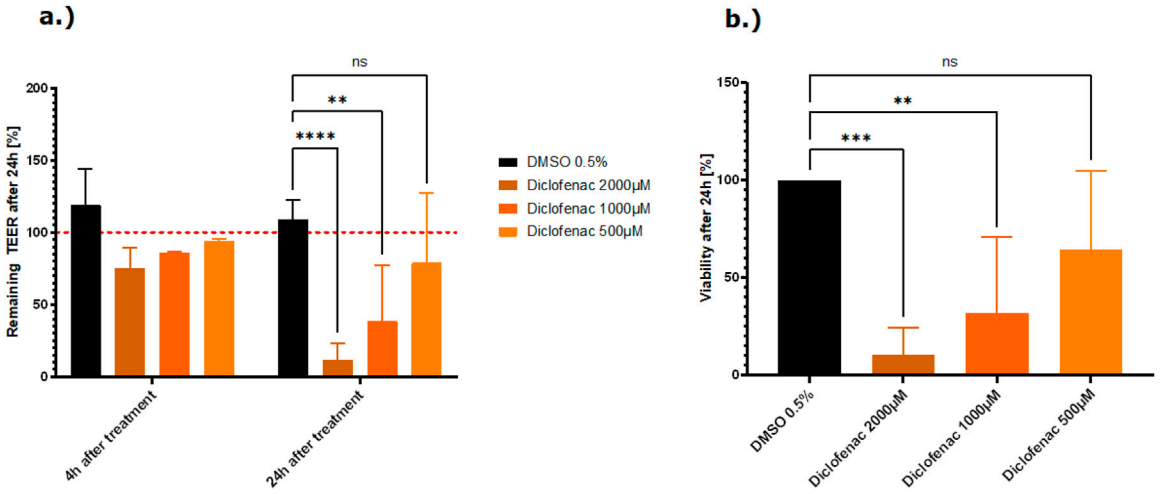


FIGURE 5
**(A)** Effect of the NSAID, diclofenac, on the barrier function shown as the percentage change relative to the TEER value at t0 of the treatment. TEER values were measured after treatment with the vehicle control DMSO and diclofenac. The mean TEER values 4 h and 24 h after treatment are shown. The dotted red line shows the normalized initial TEER values of 100%. **(B)** Effect of the NSAID, diclofenac, on the cell viability shown as a % change to the DMSO control. Viability was measured with the CellTiter-Glo 3D kit 24 h after treatment with diclofenac. The data are presented as means ± SD [n of controls = 8, n of diclofenac = 3 (2), statistical analysis of TEER values: ****$p < 0.0001$, **$p = 0.0078$, and *$p = 0.0241$ by two-way ANOVA with Dunnett's test for multiple comparisons to the control. For statistical analysis of viability values: ****$p < 0.0001$ and ***$p = 0.0010$ by one-way ANOVA with Dunnett's test for multiple comparisons to the control].

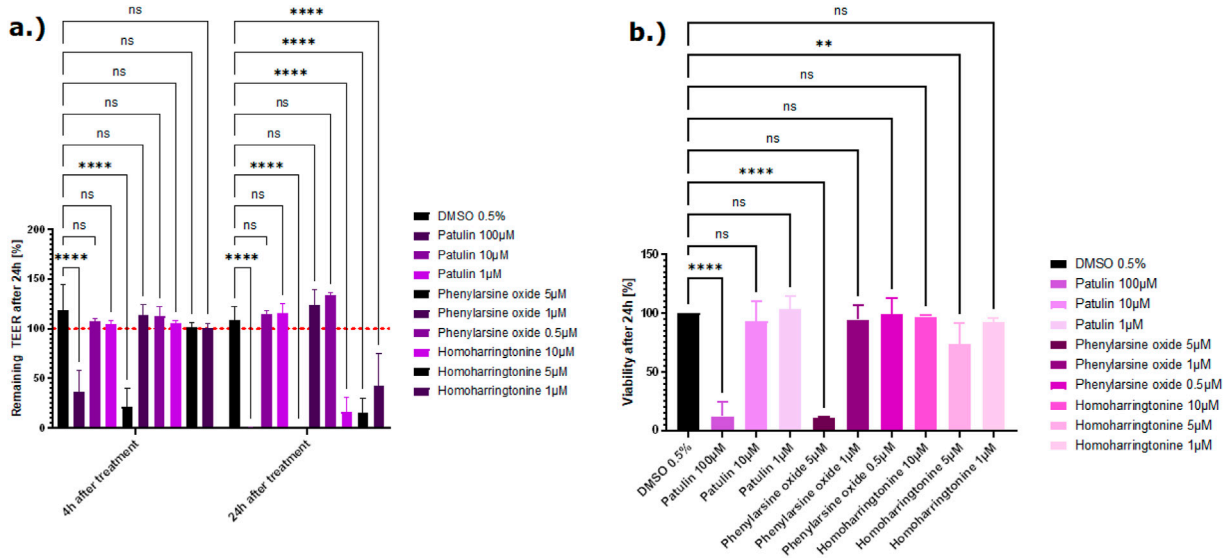


FIGURE 6
**(A)** Effect of three compounds from the tight junction damager group on the barrier function shown as the percentage change relative to the TEER value at t0 of the treatment. TEER values were measured after treatment with the vehicle control DMSO, patulin, phenylarsine oxide, and homoharringtonine. The mean TEER values 4 h and 24 h after treatment are shown. The dotted red line shows the normalized initial TEER values of 100%. **(B)** The effect of three compounds from the tight junction damager group on the cell viability shown as % change to the DMSO control. Viability was measured with the CellTiter-Glo 3D kit 24 h after treatment with patulin, phenylarsine oxide, and homoharringtonine. The data are represented as means ± SD (n of controls = 8, n of patulin = 4, n of phenylarsine oxide = 2, and n of homoharringtonine = 3; statistical analysis of TEER values: ****$p <$ 0.0001 and **$p = 0.0088$ (phenylarsine oxide), 0.0070 (10 µM homoharringtonine, and 0.0074 (5 µM homoharringtonine) by two-way ANOVA with Dunnett's test for multiple comparisons to the control. For statistical analysis of viability values: ****$p < 0.0001$ and **$p = 0.0072$ by one-way ANOVA with Dunnett's test for multiple comparisons to the control).

Transwell experiments. Table 5 shows that three of nine compounds (loperamide, afatinib, and terfenadine) lead to a decrease of the TEER values, and the other six compounds (ibuprofen, indomethacin, 5-FU, alosetron, flavopiridol, and troglitazone) did not influence the tight junctions. Their TEER values remained stable.

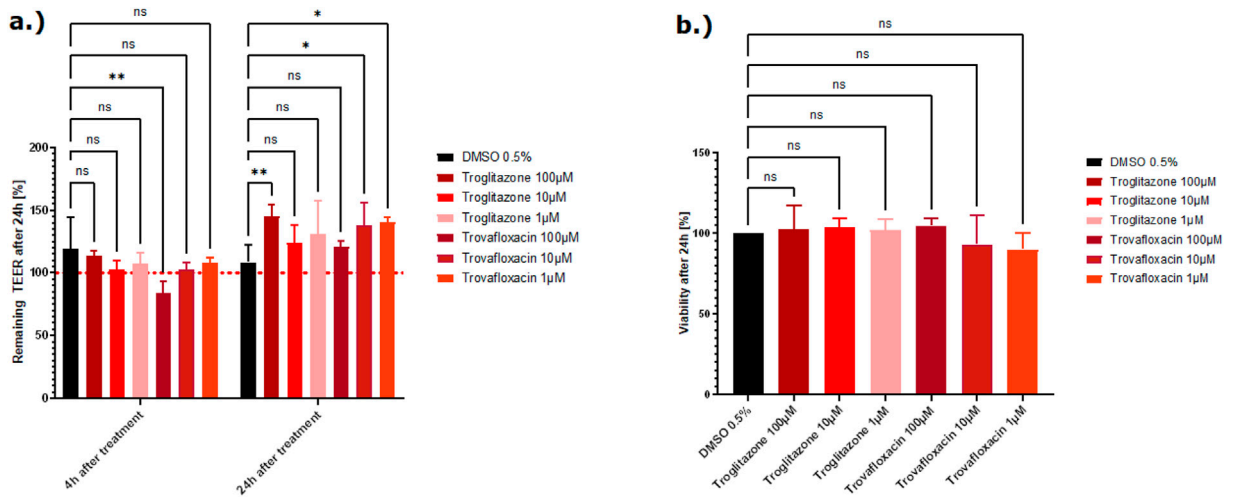


FIGURE 7
**(A)** Effect of the two liver toxins on the barrier function shown as the percentage change relative to the TEER value at t0 of the treatment. TEER values were measured after treatment with the vehicle control DMSO, troglitazone, and trovafloxacin. The mean TEER values 4 h and 24 h after treatment are shown. The dotted red line shows the normalized initial TEER values of 100%. **(B)** The effect of the two liver toxins on the cell viability shown as the percentage change relative to the DMSO control. Viability was measured with the CellTiter-Glo 3D kit 24 h after treatment with troglitazone and trovafloxacin. The data are represented as means ± SD (n of controls = 8, n of troglitazone and trovafloxacin = 3, statistical analysis of TEER values: $*p = 0.0389$ and $**p = 0.0013$ by two-way ANOVA with Dunnett's test for multiple comparisons to the control. For statistical analysis of viability values: one-way ANOVA with Dunnett's test for multiple comparisons to the control).

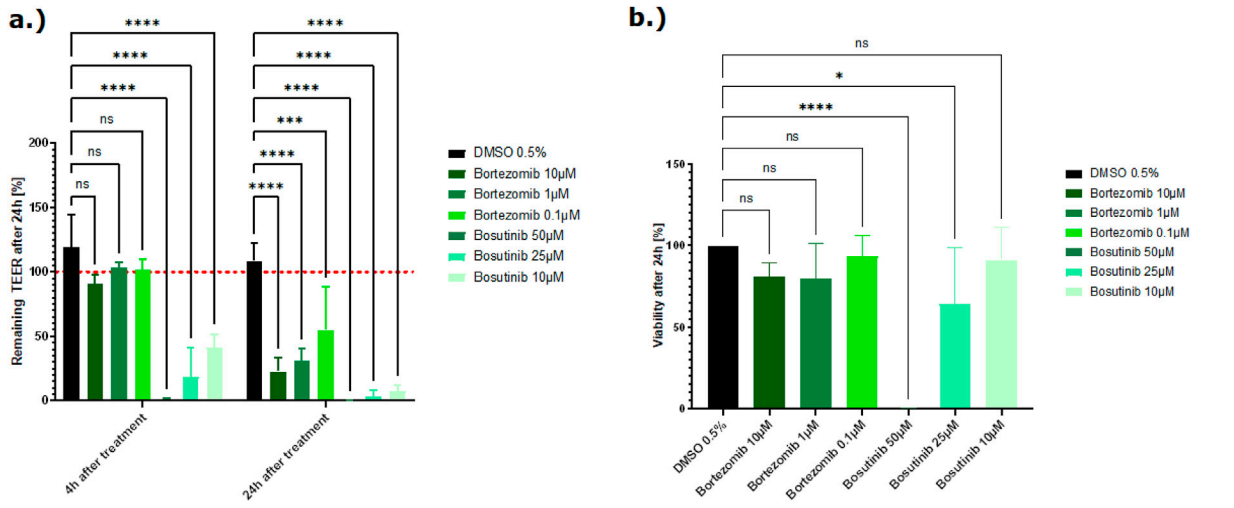


FIGURE 8
**(A)** Effect of two chemotherapeutic compounds on the barrier function shown as the percentage change relative to the TEER value at t0 of the treatment. TEER values were measured after treatment with the vehicle control DMSO, bortezomib, and bosutinib. The mean TEER values 4 h and 24 h after treatment are shown. The dotted red line shows the normalized initial TEER values of 100%. **(B)** Effect of two chemotherapeutic compounds on the cell viability shown as % change to the DMSO control. Viability was measured with the CellTiter-Glo 3D kit 24 h after treatment with bortezomib and bosutinib. The data are represented as means ± SD (n of controls = 8, n of bortezomib and bosutinib = 3, statistical analysis of TEER values: $****p < 0.0001$, $***p = 0.0005$ (10 µM bortezomib), $***p = 0.0003$ (1 µM bortezomib), and $* p = 0.0125$ by two-way ANOVA with Dunnett's test for multiple comparisons to the control. For statistical analysis of viability values: $****p < 0.0001$ and $*p = 0.0154$ by one-way ANOVA with Dunnett's test for multiple comparisons to the control).

## Discussion and conclusion

The OrganoPlate® 3-lane is a microfluidic, 3D cell culture platform that supports the differentiation and cultivation of Caco-2 cells in a tubular structure within 6 days. The medium flow, the cells being grown as 3D structures against a collagen layer, and the fast differentiation of Caco-2 cells to small intestine-like enterocytes highlight the uniqueness of this model compared to commercially available 2D Transwell models. The OrganoTEER allows sensitive, real-time interrogation of compound effects on the integrity of the intestinal barrier in a throughput suitable

TABLE 4 Overview of the TEER and viability results of the tested reference compounds (highest concentration tested). The TEER values 4 h and 24 h after treatment with the highest tested concentration of each compound are shown, reported as a percentage of the initial TEER values.

| Compound class | Compound name | Start TEER [%] | 4 h TEER [%] | End (24 h) TEER [%] | Viability decrease? | TEER decrease? | Predictivity (TEER) | Reference |
|---|---|---|---|---|---|---|---|---|
| Controls | Metformin 750 µM (neg. control) | 100 | 105.4 | 114.6 | No | No | Yes | — |
| | DMSO 0.5% (vehicle control) | 100 | 105.6 | 108.6 | No | No | Yes | — |
| | Staurosporine 100 µM (pos. control) | 100 | 16.49 | 0.4 | Yes | Yes | Yes | Trietsch et al. (2017) |
| NSAID | Ibuprofen 300 µM | 100 | 124.5 | 100.0 | No | No | No | Rampal et al. (2002) |
| | Diclofenac 2,000 µM | 100 | 75.05 | 11.8 | Yes | Yes | Yes | Bhatt et al. (2018) |
| | Indomethacin 500 µM | 100 | 77.57 | 56.2 | No | Yes | Yes | Fuentes et al. (2022) |
| Chemotherapeutics | 5-Fluorouracil 300 µM | 100 | 109.0 | 106.4 | No | No | No | Soares et al. (2013), Song et al. (2013), and Garcia-Hernandez et al. (2017) |
| | Alosetron 300 µM | 100 | 120.9 | 125.3 | No | No | No | Camilleri et al. (2001) |
| | Irinotecan 1,000 µM | 100 | 103.43 | 88.2 | No | No | No | Wardill et al. (2014) |
| | Sunitinib 5 µM | 100 | 109.6 | 132.2 | No | No | No | Durand et al. (2012) |
| | Sorafenib 25 µM | 100 | 98.9 | 115.1 | Yes | No | No | Durand et al. (2012) |
| | Flavopiridol 300 µM | 100 | 82.6 | 45.9 | No | Yes | Yes | Byrd et al. (2007) |
| | Bortezomib 10 µM | 100 | 106.1 | 24.9 | No | Yes | Yes | Sun et al., 2005; Peters et al., 2019 |
| | Bosutinib 50 µM | 100 | 1.1 | 0.1 | Yes | Yes | Yes | French (2019) |
| | Carboplatin 100 µM | 100 | 102.3 | 122.5 | No | No | No | Peters et al. (2019) |
| | Docetaxel 100 µM | 100 | 115.7 | 76.2 | No | Yes | Yes | Peters et al. (2019) |
| | Afatinib 100 µM | 100 | 50.9 | 0.7 | Yes | Yes | Yes | Peters et al. (2019) |
| Liver toxins | Troglitazone 100 µM | 100 | 108.3 | 132.8 | No | No | Yes | — |
| | Trovafloxacin 100 µM | 100 | 84.0 | 121.1 | No | No | Yes | — |
| Tight junction damager | Phenylarside oxide 5 µM | 100 | 21.2 | 0.4 | Yes | Yes | Yes | Rao et al. (1997) |
| | Sodium orthovanadate 50 µM | 100 | 129.6 | 130.5 | No | No | No | Rao et al. (1997) |
| | Homoharringtonine 10 µM | 100 | 105.8 | 16.4 | No | Yes | Yes | Watari et al. (2015) |
| | Patulin 100 µM | 100 | 36.1 | 0.3 | Yes | Yes | Yes | Mahfoud et al. (2002) |
| Mixed | Duloxetine 100 µM | 100 | 68.5 | 30.9 | Yes | Yes | Yes | Peters et al. (2019) |
| | Loperamide 300 µM | 100 | 0.3 | 0.0 | Yes | Yes | Yes | Emc (2018) |
| | Terfenadine 200 µM | 100 | 0.1 | 0.1 | Yes | Yes | Yes | Nonnenmacher (2021) |

for early preclinical safety assessment. The use of cell lines such as Caco-2 cells in MPS models is, of course, a widely discussed topic. It is well known that genetic variations between Caco-2 clones can influence the predictability of drug-induced organ damage. To minimize this, only one Caco-2 clone was used throughout the study. Cancer cell lines differ from primary intestinal cells in terms of their physiology, the expression of drug transporters, and their metabolic activity, which limits their use in *in vitro* models. It is, therefore, possible to use more physiologically relevant cell resources, such as additional cell type(s), to generate a co-culture platform (e.g., with HT29-MTX cells to simulate the mucus barrier) or by seeding iPSC/adult stem cell-derived-gut organoids to improve predictability.

Overall, 23 reference compounds were used to evaluate the applicability of the OrganoPlate® (with Caco-2 cells) in

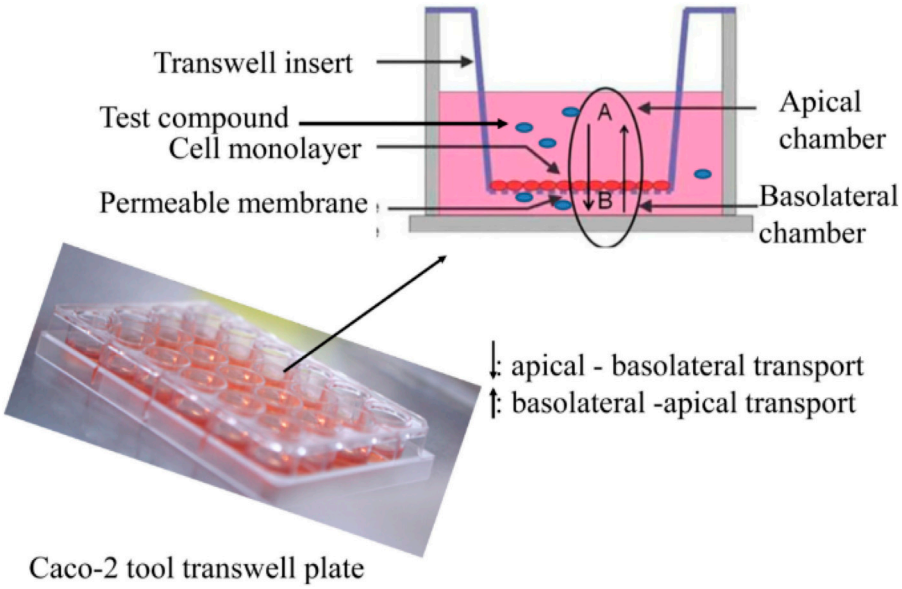


FIGURE 9
Cultivation of Caco-2 cells on permeable membranes of Transwell inserts for Transwell experiments (Awortwe et al., 2014).

combination with the OrganoTEER to determine toxic effects on the intestinal barrier. However, not all tested compounds showed damage to the tight junctions and a corresponding reduction of the TEER value. At least at the highest concentration tested, 15 of 23 compounds showed the expected outcome, which means either a decrease in TEER value in parallel to a decreased viability after the treatment, a decrease in TEER value without a reduction of the viability, or a stable TEER value and no viability loss (Table 5).

The best predictivity was shown for the NSAIDs, those that created tight junction damage, and the compounds that induce GI adverse effects *in vivo* (in each class, two of three compounds showed a decreased TEER value). For example, we were able to show that TEER values were reduced after treatment with the NSAID diclofenac, which indicates increased intestinal permeability. Consistent with a previous report, diclofenac can reduce TEER values, which indicates damaged tight junction connections and increased intestinal permeability (Bhatt et al., 2018).

Chemotherapeutic compounds are known to induce multiple adverse effects, including impacting the GI system, such as nausea, vomiting (Amjad et al., 2023) or diarrhea, pain, and constipation (Lee et al., 2014; McQuade et al., 2016; Forsgård et al., 2017). Diarrhea is often correlated with intestinal barrier damage, and in 2019, Peters et al. published a method that uses a human GI microtissue and TEER to investigate the tightness of the intestinal barrier and predict diarrhea. They showed that drugs with a very high probability of causing diarrhea in the clinic, like afatinib and idarubicin, with respectively 96% and 73% diarrhea incidence, correlate with a decrease in the TEER value and a disruption of the barrier (Peters et al., 2019). Our experiments showed the same results for afatinib, with decreased TEER values, indicating damage to the tight junctions that results in increased intestinal permeability, which indicates diarrhea. The viability of the cells was also reduced after treatment with the two highest concentrations, suggesting that this effect may be driven by direct cytotoxicity. Some differences between the results from Peters et al. and our results can be explained by the use of different cell sources. Peters et al. used different epithelial cell types with a supporting fibroblast layer for their experiment, whereas in our study, the Caco-2 cell line was used. A supporting fibroblast layer can contribute to the overall functionality of the cell model and, consequently, the toxic response to treatment. Another explanation could be that the use of ECMs in the OrganoPlate® model can influence chemotherapy resistance. Cell adhesion to collagen IV, as used in this study, may lead to an enhancement of tumorigenicity, leading to resistance to apoptosis, which can mask the toxic properties of the chemotherapeutics (Rintoul and Sethi, 2002).

Our data show that the OrganoPlate® is only partially able to detect the damage to the intestinal barrier with chemotherapeutics. Only five of the eleven chemotherapeutics led to a reduction in TEER values. No effect on the intestinal barrier was observed with the other chemotherapeutics tested in either the OrganoPlate or the Transwell systems. This can have different causes. For example, low predictivity in this context may be due to the treatment time. Chemotherapeutics have been developed to treat cancer cells, which usually have a very rapid division rate. In order to effectively treat this rapid proliferation, which can take several weeks to months, depending on the type and severity of the cancer, it is necessary to treat the cells several times. For example, colon cancer patients usually receive 4–6 months of chemotherapy (Sgouros et al., 2015), which also increases the potential toxicity due to the long treatment with chemotherapeutics. In addition, some compounds only become toxic through metabolism in the liver and thus do not show direct toxicity in the intestinal cells. Irinotecan, for example, is metabolized to a toxic metabolite, SN-38, and exposure to this active metabolite is correlated with diarrhea (Sun et al., 2020). It is clear such metabolism is missing in the two GI *in vitro* models assessed here, and therefore, no direct toxicity is to be expected.

To demonstrate that the system does not produce false positives, specific compounds that induce liver injury, trovafloxacin and troglitazone (Graham et al., 2003), were also tested. Both compounds did not affect the tight junctions in the validation

TABLE 5 Comparison of the TEER results from the OrganoPlate® and Transwell experiments and final evaluation of predictivity.

| Compound | OrganoPlate® (OP) | | | Transwell (TW) | | | OP vs. TW |
|---|---|---|---|---|---|---|---|
| | Start TEER [%] | End TEER [%] | TEER decrease? | Start TEER [%] | End TEER [%] | TEER decrease? | Predictivity |
| Metformin 750 µM (neg. control) | 100 | 114.6 | No | 100 | 106.9 | No | OP = TW |
| DMSO 0.5% (vehicle control) | 100 | 108.6 | No | 100 | 103.1 | No | OP = TW |
| Staurosporine 10 µM (pos. control TEER) | 100 | 1.7 | Yes | 100 | 10.8 | Yes | OP = TW |
| Ibuprofen 300 µM | 100 | 100.0 | No | 100 | 108.5 | No | OP = TW |
| Diclofenac 2000 µM | 100 | 11.8 | Yes | NA | NA | NA | NA |
| Indomethacin 500 µM | 100 | 56.2 | Yes | 100 | 82.5 | No | OP > TW |
| 5-Fluorouracil 300 µM | 100 | 106.4 | No | 100 | 90.1 | No | OP = TW |
| Alosetron 300 µM | 100 | 125.3 | No | 100 | 131.5 | No | OP = TW |
| Irinotecan 1000 µM | 100 | 88.2 | No | NA | NA | NA | NA |
| Sunitinib 5 µM | 100 | 132.2 | No | NA | NA | NA | NA |
| Sorafenib 25 µM | 100 | 115.1 | No | NA | NA | NA | NA |
| Flavopiridol 300 µM | 100 | 45.9 | Yes | 100 | 80.6 | No | OP > TW |
| Bortezomib 10 µM | 100 | 24.9 | Yes | NA | NA | NA | NA |
| Bosutinib 50 µM | 100 | 0.1 | Yes | NA | NA | NA | NA |
| Carboplatin 100 µM | 100 | 122.5 | No | NA | NA | NA | NA |
| Docetaxel 100 µM | 100 | 76.2 | Yes | NA | NA | NA | NA |
| Afatinib 100 µM | 100 | 0.7 | Yes | 100 | 76.5 | yes | OP > TW |
| Troglitazone 100 µM | 100 | 132.8 | No | 100 | 96.4 | no | OP = TW |
| Trovafloxacin 100 µM | 100 | 121.1 | No | NA | NA | NA | NA |
| Phenylarside oxide 5 µM | 100 | 0.4 | Yes | NA | NA | NA | NA |
| Sodium orthovanadate 50 µM | 100 | 130.5 | No | NA | NA | NA | NA |
| Homoharringtonine 10 µM | 100 | 16.4 | Yes | NA | NA | NA | NA |
| Patulin 100 µM | 100 | 0.3 | Yes | NA | NA | NA | NA |
| Duloxetine 100 µM | 100 | 30.9 | Yes | NA | NA | NA | NA |
| Loperamide 300 µM | 100 | 0.0 | Yes | 100 | 5.9 | yes | OP = TW |
| Terfenadine 200 µM | 100 | 0.1 | Yes | 100 | 4.4 | yes | OP = TW |

experiments nor decrease the viability of the Caco-2 cells (Figures 7A, B), which supports the ability to correctly predict GI non-toxic compounds. No GI-related toxicities have been reported for troglitazone (Klopotek et al., 2006).

Phenylarsine oxide, patulin, sodium orthovanadate, and homoharringtonine are all known to disrupt the tight junctions by either inhibiting protein tyrosine phosphatase, a key regulator of intestinal epithelial barrier function (Rao et al., 1997; Mahfoud et al., 2002) or by downregulating the claudine 3 and 4 expression. A disturbed localization of claudine 3 and 4 impairs the barrier formation (Watari et al., 2015) that is essential for the function of the intestine. Clinically, patulin is known to induce intestinal epithelial cell degeneration, ulceration, hemorrhages, and inflammation (Mahfoud et al., 2002) and leads to phosphorylation of claudin-4 and occluding, which causes degradation of the ZO-1 protein (Kawauchiya et al., 2011) and can lead to damage to tight junctions.

In our experiments, phenylarsine, patulin, and homoharringtonine decreased the TEER values in the OrganoPlate®, which indicated a damaged barrier. No data on these three substances could be collected for the 2D Transwell model to date.

The comparison of the results from the Transwell experiments and the OrganoPlate® experiments shows that the OrganoPlate® is more reliable in its ability to predict GI toxicity. The traditional Transwell was at least as predictive for intestinal barrier damage as the OrganoPlate® for three of the tested compounds. However, it is clear from our data that the Transwell model is not a suitable option for most of the other substances tested here, as it could not predict the toxic properties of the compounds on the intestinal barrier. In addition, indomethacin,

flavopiridol, and afatinib led to a stronger decrease in the TEER value in the OrganoPlate® than in the Transwell system. After using the Transwell system, these compounds would have been classified as non-toxic, whereas the OrganoPlate® was able to demonstrate clear damage to the intestinal barrier.

The TEER measurement is a reliable and widely accepted quantitative technique to identify the integrity of tight junctions of cell culture barriers (Srinivasan et al., 2015). The present findings demonstrate that the measurement of TEER with the OrganoPlate® can be used for the early safety prediction of drug-induced damage on the intestinal barrier. The OrganoPlate® includes several features that are important for early preclinical drug screening: (a) 3D tubular structure of cells that mimics the intestinal system itself, (b) sufficient throughput (40 chips), (c) shorter pre-cultivation time than cell models on Transwell inserts (21 days pre-cultivation), and (d) a functional endpoint that enables distinguishing between drug-induced damage on the intestinal barrier (tight junctions) and cytotoxicity of the enterocytes. The data reported here help the qualification of the OrganoPlate® as a routine test system for the early prediction of drug-induced GI toxicity. Looking to the future, it is conceivable that the OrganoPlate® could be used for other context-of-use cases: for example, experiments to determine drug–drug interaction, testing active metabolites of drugs, or use later in the development cycle for more mechanistic questions.

## Data availability statement

The raw data supporting the conclusions of this article will be made available by the authors, without undue reservation.

## Ethics statement

Ethical approval was not required for the studies on humans in accordance with the local legislation and institutional requirements because only commercially available established cell lines were used.

## Author contributions

SH: data curation, investigation, methodology, software, validation, visualization, writing–original draft, writing–review and editing, conceptualization, and formal analysis. PH: conceptualization, funding acquisition, project administration, resources, supervision, writing–review and editing, and validation. IK: investigation and writing–review and editing. DK: writing–review and editing and resources. WS: resources and writing–review and editing. KK: writing–review and editing and resources.

## Funding

The author(s) declare that financial support was received for the research, authorship, and/or publication of this article. This work was supported by Mimetas.

## Acknowledgments

The authors thank the following colleagues for their kind contribution to this work: A. Augustin and J. Langer.

## Conflict of interest

Authors SH, PH, and IK were employed by Merck Healthcare KGaA. Authors DK, WS, and KK were employed by MIMETAS B.V.

## Publisher's note

All claims expressed in this article are solely those of the authors and do not necessarily represent those of their affiliated organizations, or those of the publisher, the editors, and the reviewers. Any product that may be evaluated in this article, or claim that may be made by its manufacturer, is not guaranteed or endorsed by the publisher.

## Supplementary material

The Supplementary Material for this article can be found online at: https://www.frontiersin.org/articles/10.3389/fddsv.2024.1459424/full#supplementary-material

## References

Amjad, M. T., Chidharla, A., and Kasi, A. (2023). *Cancer chemotherapy. StatPearls*. Treasure Island (FL): StatPearls Publishing. Copyright © 2023, StatPearls Publishing LLC.

Antonsson, A., and Persson, J. L. (2009). Induction of apoptosis by staurosporine involves the inhibition of expression of the major cell cycle proteins at the $G_2$/M checkpoint accompanied by alterations in erk and akt kinase activities. *Anticancer Res.* 29 (8), 2893–2898.

Awortwe, C., Fasinu, P. S., and Rosenkranz, B. (2014). Application of Caco-2 cell line in herb-drug interaction studies: current approaches and challenges. *J. Pharm. Pharm. Sci.* 17 (1), 1–19. doi:10.18433/j30k63

Ayehunie, S. S. Z., Landry, T., Armento, A., Klausner, M., and Hayden, P. J. (2013). A new organotypic 3-D small intestinal tissue model reconstructed from primary human cells. *Toxicol. Lett.* 221, S88. doi:10.1016/j.toxlet.2013.05.108

Benson, K., Cramer, S., and Galla, H. J. (2013). Impedance-based cell monitoring: barrier properties and beyond. *Fluids Barriers CNS* 10 (1), 5. doi:10.1186/2045-8118-10-5

Bhatt, A. P., Gunasekara, D. B., Speer, J., Reed, M. I., Peña, A. N., Midkiff, B. R., et al. (2018). Nonsteroidal anti-inflammatory drug-induced leaky gut modeled using polarized monolayers of primary human intestinal epithelial cells. *ACS Infect. Dis.* 4 (1), 46–52. doi:10.1021/acsinfecdis.7b00139

Bonnet, F., and Scheen, A. (2017). Understanding and overcoming metformin gastrointestinal intolerance. *Diabetes Obes. Metab.* 19 (4), 473–481. doi:10.1111/dom.12854

Byrd, J. C., Lin, T. S., Dalton, J. T., Wu, D., Phelps, M. A., Fischer, B., et al. (2007). Flavopiridol administered using a pharmacologically derived schedule is associated with marked clinical efficacy in refractory, genetically high-risk chronic lymphocytic leukemia. *Blood* 109 (2), 399–404. doi:10.1182/blood-2006-05-020735

Camilleri, M., Chey, W. Y., Mayer, E. A., Northcutt, A. R., Heath, A., Dukes, G. E., et al. (2001). A randomized controlled clinical trial of the serotonin type 3 receptor antagonist alosetron in women with diarrhea-predominant irritable bowel syndrome. *Arch. Intern Med.* 161 (14), 1733–1740. doi:10.1001/archinte.161.14.1733

Crystal, M. (2018). Pros and cons of animal testing. Available at: https://sciencing.com/importance-animals-human-lives-5349359.html.

Durand, J. B., Buyse, M., Neveux, N., Boudou-Rouquette, P., Mir, O., Vidal, M., et al. (2012). Relationship between intestinal function and exposure to sorafenib and sunitinib in cancer patients. *Ann. Oncol.* 23 (9), ix91. doi:10.1016/s0923-7534(20)32797-6

EMC (2018). Irinotecan hydrochloride 20 mg/ml concentrate for solution for infusion. Available at: https://www.medicines.org.uk/emc/product/6506/smpc.

Forsgård, R. A., Marrachelli, V. G., Korpela, K., Frias, R., Collado, M. C., Korpela, R., et al. (2017). Chemotherapy-induced gastrointestinal toxicity is associated with changes in serum and urine metabolome and fecal microbiota in male Sprague-Dawley rats. *Cancer Chemother. Pharmacol.* 80 (2), 317–332. doi:10.1007/s00280-017-3364-z

French, A. (2019). *Mechanisms of lower gastrointestinal toxicity caused by tyrosine kinase inhibitors*. Liverpool: Doctor of Philosophy.

Fuentes, J., Brunser, O., Atala, E., Herranz, J., de Camargo, A. C., Zbinden-Foncea, H., et al. (2022). Protection against indomethacin-induced loss of intestinal epithelial barrier function by a quercetin oxidation metabolite present in onion peel: *in vitro* and *in vivo* studies. *J. Nutr. Biochem.* 100, 108886. doi:10.1016/j.jnutbio.2021.108886

Garcia-Hernandez, V., Quiros, M., and Nusrat, A. (2017). Intestinal epithelial claudins: expression and regulation in homeostasis and inflammation. *Ann. N. Y. Acad. Sci.* 1397 (1), 66–79. doi:10.1111/nyas.13360

Graham, D. J., Green, L., Senior, J. R., and Nourjah, P. (2003). Troglitazone-induced liver failure: a case study. *Am. J. Med.* 114 (4), 299–306. doi:10.1016/s0002-9343(02)01529-2

Hanauer, S. B. (2008). The role of loperamide in gastrointestinal disorders. *Rev. Gastroenterol. Disord.* 8 (1), 15–20.

Ho, M. Y., and Mackey, J. R. (2014). Presentation and management of docetaxel-related adverse effects in patients with breast cancer. *Cancer Manag. Res.* 6, 253–259. doi:10.2147/CMAR.S40601

Kawauchiya, T., Takumi, R., Kudo, Y., Takamori, A., Sasagawa, T., Takahashi, K., et al. (2011). Correlation between the destruction of tight junction by patulin treatment and increase of phosphorylation of ZO-1 in Caco-2 human colon cancer cells. *Toxicol. Lett.* 205 (2), 196–202. doi:10.1016/j.toxlet.2011.06.006

Khoury, H. J., Cortes, J. E., Kantarjian, H. M., Gambacorti-Passerini, C., Baccarani, M., Kim, D. W., et al. (2012). Bosutinib is active in chronic phase chronic myeloid leukemia after imatinib and dasatinib and/or nilotinib therapy failure. *Blood* 119 (15), 3403–3412. doi:10.1182/blood-2011-11-390120

Kim, H. G., Jeong, S. G., Kim, J. H., and Cho, J. Y. (2022). Phosphatase inhibition by sodium orthovanadate displays anti-inflammatory action by suppressing AKT-IKKβ signaling in RAW264.7 cells. *Toxicol. Rep.* 9, 1883–1893. doi:10.1016/j.toxrep.2022.09.012

Klopotek, A., Hirche, F., and Eder, K. (2006). PPARγ ligand troglitazone lowers cholesterol synthesis in HepG2 and caco-2 cells via a reduced concentration of nuclear SREBP-2. *Exp. Biol. Med.* 231 (8), 1365–1372. doi:10.1177/153537020623100810

Lee, C. S., Ryan, E. J., and Doherty, G. A. (2014). Gastro-intestinal toxicity of chemotherapeutics in colorectal cancer: the role of inflammation. *World J. Gastroenterol.* 20 (14), 3751–3761. doi:10.3748/wjg.v20.i14.3751

Lee, S. H. (2015). Intestinal permeability regulation by tight junction: implication on inflammatory bowel diseases. *Intest. Res.* 13 (1), 11–18. doi:10.5217/ir.2015.13.1.11

Lemmens, G., Van Camp, A., Kourula, S., Vanuytsel, T., and Augustijns, P. (2021). Drug disposition in the lower gastrointestinal tract: targeting and monitoring. *Pharmaceutics* 13 (2), 161. doi:10.3390/pharmaceutics13020161

Le Tourneau, C., Raymond, E., and Faivre, S. (2007). Sunitinib: a novel tyrosine kinase inhibitor. A brief review of its therapeutic potential in the treatment of renal carcinoma and gastrointestinal stromal tumors (GIST). *Ther. Clin. Risk Manag.* 3 (2), 341–348. doi:10.2147/tcrm.2007.3.2.341

Mahfoud, R., Maresca, M., Garmy, N., and Fantini, J. (2002). The mycotoxin patulin alters the barrier function of the intestinal epithelium: mechanism of action of the toxin and protective effects of glutathione. *Toxicol. Appl. Pharmacol.* 181 (3), 209–218. doi:10.1006/taap.2002.9417

Maseda, D., and Ricciotti, E. (2020). NSAID-gut microbiota interactions. *Front. Pharmacol.* 11, 1153. doi:10.3389/fphar.2020.01153

McQuade, R. M., Stojanovska, V., Abalo, R., Bornstein, J. C., and Nurgali, K. (2016). Chemotherapy-induced constipation and diarrhea: pathophysiology, current and emerging treatments. *Front. Pharmacol.* 7, 414. doi:10.3389/fphar.2016.00414

Mellstrand, T. (1987). Loperamide—an opiate receptor agonist with gastrointestinal motility effects. *Scand. J. Gastroenterology* 22 (Suppl. 130), 65–66. doi:10.3109/00365528709091001

Nicolas, A. S. F., Kosim, K., Kurek, D., Haarmans, M., Bulst, M., Lee, K., et al. (2021). High throughput transepithelial electrical resistance (TEER) measurements on perfused membrane-free epithelia. *R. Soc. Chem.* 21, 1676–1685. doi:10.1039/D0LC00770F

Nonnenmacher, (2021). *Terfenadin - Wirkung*. Anwendung & Risiken | MedLexi.de. Available at: https://medlexi.de/Terfenadin (Accessed October 26, 2021).

Oikawa, T., Shimamura, M., Ashino, H., Nakamura, O., Kanayasu, T., Morita, I., et al. (1992). Inhibition of angiogenesis by staurosporine, a potent protein kinase inhibitor. *J. antibiotics* 45 (7), 1155–1160. doi:10.7164/antibiotics.45.1155

Paone, P., and Cani, P. D. (2020). Mucus barrier, mucins and gut microbiota: the expected slimy partners? *Gut* 69 (12), 2232–2243. doi:10.1136/gutjnl-2020-322260

Peng, W., Datta, P., Ayan, B., Ozbolat, V., Sosnoski, D., and Ozbolat, I. T. (2017). 3D bioprinting for drug discovery and development in pharmaceutics. *Acta Biomater.* 57, 26–46. doi:10.1016/j.actbio.2017.05.025

Peters, M. F., Landry, T., Pin, C., Maratea, K., Dick, C., Wagoner, M. P., et al. (2019). Human 3D gastrointestinal microtissue barrier function as a predictor of drug-induced diarrhea. *Toxicol. Sci.* 168 (1), 3–17. doi:10.1093/toxsci/kfy268

Rainsford, K. D. (2009). Ibuprofen: pharmacology, efficacy and safety. *Inflammopharmacology* 17 (6), 275–342. doi:10.1007/s10787-009-0016-x

Rampal, P., Moore, N., Van Ganse, E., Le Parc, J. M., Wall, R., Schneid, H., et al. (2002). Gastrointestinal tolerability of ibuprofen compared with paracetamol and aspirin at over-the-counter doses. *J. Int. Med. Res.* 30 (3), 301–308. doi:10.1177/147323000203000311

Rao, R. K., Baker, R. D., Baker, S. S., Gupta, A., and Holycross, M. (1997). Oxidant-induced disruption of intestinal epithelial barrier function: role of protein tyrosine phosphorylation. *Am. J. Physiology-Gastrointestinal Liver Physiology* 273 (4), G812–G823. doi:10.1152/ajpgi.1997.273.4.G812

Rena, G., Hardie, D. G., and Pearson, E. R. (2017). The mechanisms of action of metformin. *Diabetologia* 60 (9), 1577–1585. doi:10.1007/s00125-017-4342-z

Rintoul, R. C., and Sethi, T. (2002). Extracellular matrix regulation of drug resistance in small-cell lung cancer. *Clin. Sci.* 102 (4), 417–424. doi:10.1042/cs1020417

Roden, D. M. (2019). A current understanding of drug-induced QT prolongation and its implications for anticancer therapy. *Cardiovasc Res.* 115 (5), 895–903. doi:10.1093/cvr/cvz013

Sambuy, Y., De Angelis, I., Ranaldi, G., Scarino, M. L., Stammati, A., and Zucco, F. (2005). The Caco-2 cell line as a model of the intestinal barrier: influence of cell and culture-related factors on Caco-2 cell functional characteristics. *Cell Biol. Toxicol.* 21 (1), 1–26. doi:10.1007/s10565-005-0085-6

Sehdev, S. (2016). Sunitinib toxicity management - a practical approach. *Can. Urol. Assoc. J.* 10 (11-12Suppl. 7), S248–s251. doi:10.5489/cuaj.4296

Senderowicz, A. M. (1999). Flavopiridol: the first cyclin-dependent kinase inhibitor in human clinical trials. *Invest New Drugs* 17 (3), 313–320. doi:10.1023/a:1006353008903

Sgouros, J., Aravantinos, G., Kouvatseas, G., Rapti, A., Stamoulis, G., Bisvikis, A., et al. (2015). Impact of dose reductions, delays between chemotherapy cycles, and/or shorter courses of adjuvant chemotherapy in stage II and III colorectal cancer patients: a single-center retrospective study. *J. Gastrointest. Cancer* 46 (4), 343–349. doi:10.1007/s12029-015-9746-8

Soares, P. M., Mota, J. M., Souza, E. P., Justino, P. F., Franco, A. X., Cunha, F. Q., et al. (2013). Inflammatory intestinal damage induced by 5-fluorouracil requires IL-4. *Cytokine* 61 (1), 46–49. doi:10.1016/j.cyto.2012.10.003

Soderholm, A. T., and Pedicord, V. A. (2019). Intestinal epithelial cells: at the interface of the microbiota and mucosal immunity. *Immunology* 158 (4), 267–280. doi:10.1111/imm.13117

Song, M. K., Park, M. Y., and Sung, M. K. (2013). 5-Fluorouracil-induced changes of intestinal integrity biomarkers in BALB/c mice. *J. Cancer Prev.* 18 (4), 322–329. doi:10.15430/jcp.2013.18.4.322

Srinivasan, B., Kolli, A. R., Esch, M. B., Abaci, H. E., Shuler, M. L., and Hickman, J. J. (2015). TEER measurement techniques for *in vitro* barrier model systems. *J. Lab. Autom.* 20 (2), 107–126. doi:10.1177/2211068214561025

Sun, K., Wilkins, D. E., Anver, M. R., Sayers, T. J., Panoskaltsis-Mortari, A., Blazar, B. R., et al. (2005). Differential effects of proteasome inhibition by bortezomib on murine acute graft-versus-host disease (GVHD): delayed administration of bortezomib results in increased GVHD-dependent gastrointestinal toxicity. *Blood* 106 (9), 3293–3299. doi:10.1182/blood-2004-11-4526

Sun, R., Zhu, L., Li, L., Song, W., Gong, X., Qi, X., et al. (2020). Irinotecan-mediated diarrhea is mainly correlated with intestinal exposure to SN-38: critical role of gut Ugt. *Toxicol. Appl. Pharmacol.* 398, 115032. doi:10.1016/j.taap.2020.115032

Thomson, A., Smart, K., Somerville, M. S., Lauder, S. N., Appanna, G., Horwood, J., et al. (2019). The Ussing chamber system for measuring intestinal permeability in health and disease. *BMC Gastroenterol.* 19 (1), 98. doi:10.1186/s12876-019-1002-4

Trietsch, S. J., Naumovska, E., Kurek, D., Setyawati, M. C., Vormann, M. K., Wilschut, K. J., et al. (2017). Membrane-free culture and real-time barrier integrity assessment of perfused intestinal epithelium tubes. *Nat. Commun.* 8 (1), 262. doi:10.1038/s41467-017-00259-3

Turner, J. R. (2009). Intestinal mucosal barrier function in health and disease. *Nat. Rev. Immunol.* 9 (11), 799–809. doi:10.1038/nri2653

Vancamelbeke, M., and Vermeire, S. (2017). The intestinal barrier: a fundamental role in health and disease. *Expert Rev. Gastroenterol. Hepatol.* 11 (9), 821–834. doi:10.1080/17474124.2017.1343143

Walter, E., Janich, S., Roessler, B. J., Hilfinger, J. M., and Amidon, G. L. (1996). HT29-MTX/Caco-2 cocultures as an *in vitro* model for the intestinal epithelium: *in vitro-in vivo* correlation with permeability data from rats and humans. *J. Pharm. Sci.* 85 (10), 1070–1076. doi:10.1021/js960110x

Wardill, H. R., Bowen, J. M., Al-Dasooqi, N., Sultani, M., Bateman, E., Stansborough, R., et al. (2014). Irinotecan disrupts tight junction proteins within the gut: implications for chemotherapy-induced gut toxicity. *Cancer Biol. Ther.* 15 (2), 236–244. doi:10.4161/cbt.27222

Watari, A., Hashegawa, M., Yagi, K., and Kondoh, M. (2015). Homoharringtonine increases intestinal epithelial permeability by modulating specific claudin isoforms in Caco-2 cell monolayers. *Eur. J. Pharm. Biopharm.* 89, 232–238. doi:10.1016/j.ejpb.2014.12.012

William, B., Mitch, A. P., Rebecca, B. K., Darlene, M. R., Wenjun, N., Katie, A. A., et al. (2010). Phase I clinical and pharmacokinetic study of a novel schedule of flavopiridol in relapsed or refractory acute leukemias. *Haematologica* 95 (7), 1098–1105. doi:10.3324/haematol.2009.017103

Zhang, Y., Huang, S., Zhong, W., Chen, W., Yao, B., and Wang, X. (2021). 3D organoids derived from the small intestine: an emerging tool for drug transport research. *Acta Pharm. Sin. B* 11 (7), 1697–1707. doi:10.1016/j.apsb.2020.12.002

Zhou, D. C., Zittoun, R., and Marie, J. P. (1995). Homoharringtonine: an effective new natural product in cancer chemotherapy. *Bull. Cancer* 82 (12), 987–995.